Review Commentary

Journal of Physical Organic Chemistry

Received: 29 December 2007, Revised: 1 March 2008, Accepted: 3 March 2008, Published online in Wiley InterScience: 9 June 2008

(www.interscience.wiley.com) DOI 10.1002/poc.1367

A mechanistic dichotomy in concerted *versus* stepwise pathways in hydride and hydrogen transfer reactions of NADH analogues

Junpei Yuasa[b] and Shunichi Fukuzumi[a*]

A mechanistic dichotomy of one-step *versus* stepwise pathways in hydride and hydrogen transfer reactions of NADH analogues is discussed including the relation between two pathways: a continuous change *versus* a discontinuous change of the mechanism. Examples of stepwise electron–proton–electron transfer through a charge transfer (CT) complex in hydride transfer from NADH analogues to hydride acceptors are presented including the detection and the reactivity of the intermediate, that is, radical cations of NADH analogues. The relation between stepwise *versus* one-step mechanisms of hydride and hydrogen transfer reaction of NADH analogues is also clarified by showing examples of the change of the mechanism including the borderline. Copyright © 2008 John Wiley & Sons, Ltd.

Keywords: electron transfer; NADH analogue; hydride transfer; hydrogen transfer; mechanistic dichotomy

INTRODUCTION

Hydride (H^-) transfer, which is equivalent to two e^- and a H^+ transfer, is essential for many biological redox processes. The biological equivalent of hydride transfer reagents is nicotinamide adenine dinucleotide (NADH) and its phosphorelated analogue, NADPH.[1] The main mechanistic issue in hydride transfer from NADH to hydride acceptor (A) is whether hydride transfer occurs in a stepwise manner by sequential electron–proton–electron transfer ($e^- + H^+ + e^-$) or a one-step transfer of hydride ion (H^-) by a concerted pathway.[2–5] The mechanistic borderline between one-step and multistep reactions has always been of a significant general interest to chemists. There has been long standing ambiguity as to the mechanistic borderline in the hydride transfer reactions of NADH and analogues (Scheme 1), although hydride transfer reaction mechanisms of NADH analogues have so far been extensively studied in reactions with various inorganic[6–15] and organic[16–33] substrates. The effects of metal ion on the mechanistic borderline in the hydride transfer reactions of NADH and analogues have also attracted interest because of the essential role of metal ions in the redox reactions of nicotinamide coenzymes in the native enzymatic system.[34–42] NADH can act both as a hydrogen donor and as a hydride donor in hydrogen transfer reactions.[1–3,43] There has also been a long standing ambiguity as to the mechanistic borderline where a one-step hydrogen transfer pathway is changed to a sequential electron and proton transfer pathway or vice versa.[44–51] A more delicate question is how two mechanisms (one-step *vs.* stepwise pathways) in hydride and hydrogen transfer reactions merge at the borderline: is there a mechanistic continuity or are both pathways employed simultaneously?

This review intends to answer these questions by focusing on a mechanistic dichotomy of one-step *versus* stepwise pathways in hydride and hydrogen transfer reactions of NADH analogues including the relation between two pathways: a continuous change *versus* a discontinuous change of the mechanism. First, a stepwise pathway via electron transfer through a charge transfer complex in hydride transfer from NADH analogues to hydride acceptors is delineated, including the detection and the reactivity of the intermediate, that is, radical cations of NADH analogues. Then, the relation between stepwise *versus* one-step mechanisms of hydride and hydrogen transfer reaction of NADH analogues is clarified by showing examples of the change of the mechanism.

STEPWISE ET PATHWAYS IN HYDRIDE TRANSFER

Hydride transfer reactions from NADH analogues, 10-methyl-9, 10-dihydroacridine ($AcrH_2$) as well as 1-benzyl-1,4-dihydronicotinamide (BNAH), to hydride acceptors (A) such as *p*-benzoquinone derivatives[25,37,52,53] and tetracyanoethylene (TCNE)[14]

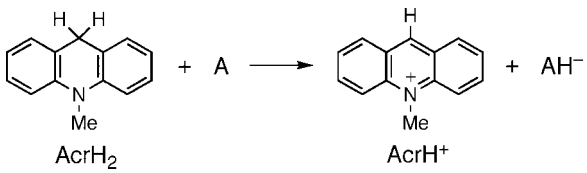

(1)

$$AH^- + A \longrightarrow AH^{\bullet} + A^{\bullet-} \quad (2)$$

$$2\,AH^{\bullet} \longrightarrow A + AH_2 \quad (3)$$

*a Correspondence to: S. Fukuzumi, Department of Material and Life Science, Graduate School of Engineering, Osaka University, SORST, Japan Science and Technology Agency, 2-1 Yamada-oka, Suita, Osaka 565-0871, Japan. E-mail: fukuzmi@chem.eng.osaka-u.ac.jp

b J. Yuasa
Graduate School of Materials Science, Nara Institute of Science and Technology, 8916-5 Takayama, Ikoma, Nara 630-0192, Japan.

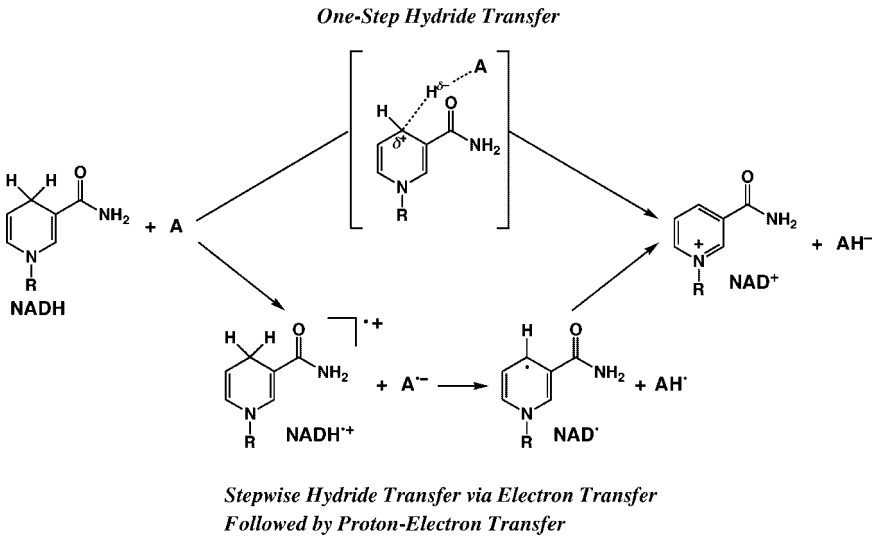

Scheme 1.

occur efficiently (Eqn (1)) followed by a subsequent fast electron transfer from the reduced product (AH^-) to A (Eqn (2)) and the disproportionation of the resulting radical (Eqn (3)).

The reactivity of 9-substituted 10-methyl-9,10-dihydroacridine (AcrHR) in the reactions with hydride acceptors (A) such as *p*-benzoquinone derivatives and TCNE in acetonitrile (MeCN) varies significantly, spanning a range of 10^7 starting from R = H to Bu^t and CMe_2COOMe, although the electron donor ability is not significantly affected by the substituent R.[54] Comparison of the large variation in the rate constant of the hydride transfer reaction (k_{obs}) with the rate constant (k_d) of the deprotonation of the radical cation ($AcrHR^{\bullet+}$) determined independently[55] is shown as linear correlations between log k_{obs} and log k_d in Fig. 1a. Such linear correlations indicate that the large variation in the reactivity is attributed mainly to that of proton transfer from $AcrHR^{\bullet+}$ to $A^{\bullet-}$ following the initial electron transfer from AcrHR to A.[52,53] The overall hydride transfer reaction from AcrHR to A, therefore, proceeds via sequential electron–proton–electron transfer, in which the initial electron transfer to give the radical ion pair ($AcrHR^{\bullet+}$ $A^{\bullet-}$) is in equilibrium and the proton transfer from $AcrHR^{\bullet+}$ to $A^{\bullet-}$ is the rate-determining step (Scheme 2).[52,53]

According to Scheme 2, the observed rate constant (k_{obs}) of the overall hydride transfer is given by Eqn (4), where $K_{et} = k_{et}/k_b$, provided that the electron transfer from $AcrR^{\bullet}$ to $AH^{\bullet}$ in the final step in Scheme 2 is much faster than the proton transfer from $AcrHR^{\bullet+}$ to $A^{\bullet-}$.[54] The fast electron transfer from $AcrH^{\bullet}$ to $AH^{\bullet}$ is well supported by

$$k_{obs} = k_p K_{et} \quad (4)$$

The highly negative one-electron oxidation potential of $AcrH^{\bullet}$ ($E_{ox} = -0.46$ V, and this is equivalent to the one-electron reduction potential of $AcrH^+$)[54] is much more negative than the one-electron reduction potential of A (E_{red} *vs.* SCE = 0.51 V and 0.22 V for DDQ and TCNE, respectively).[37,56] However, the equilibrium constant for electron transfer from AcrHR to A (K_{et}) to produce free $AcrHR^{\bullet+}$ and $A^{\bullet-}$ can be obtained from the E_{ox} value of AcrHR and the E_{red} value of A by Eqn (5). When the difference in the K_{et} values for the AcrHR-DDQ and AcrHR-TCNE systems,

$$K_{et} = \exp[-F(E_{ox} - E_{red})/RT] \quad (5)$$

is taken into account in the plots between log k_{obs} and log k_d, the two separate linear correlations and deviation from the linear lines in Fig. 1a are remarkably merged into a single line with a slope of unity in plots of log k_{obs} *versus* log $k_d K_{et}$ (Fig. 1b).[54] Such a merged single linear correlation in Fig. 1b clearly demonstrates that the hydride transfer from AcrHR to A proceeds via sequential

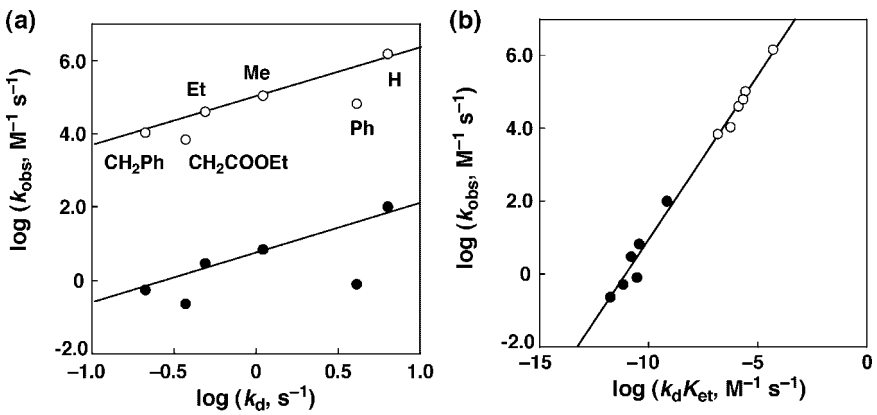

Figure 1. (a) Plots of k_{obs} for the reaction of AcrHR with DDQ (○) and TCNE (●) *versus* k_d for deprotonation of $AcrHR^{\bullet+}$ in MeCN at 298 K.[54] (b) Plots of k_{obs} for the reaction of AcrHR with DDQ (○) and TCNE (●) *versus* $k_d K_{et}$[54]

$$\mathrm{AcrHR} + \mathrm{A} \underset{k_b}{\overset{k_{et}}{\rightleftharpoons}} \left(\mathrm{AcrHR}^{\bullet+}\ \mathrm{A}^{\bullet-}\right) \xrightarrow{k_p} \left(\mathrm{AcrR}^{\bullet}\ \mathrm{AH}^{\bullet}\right) \xrightarrow{\text{fast}} \mathrm{AcrR}^{+} + \mathrm{AH}^{-}$$

Scheme 2.

electron–proton–electron transfer in which the initial electron transfer is in equilibrium and the proton transfer from $AcrHR^{\bullet+}$ to $A^{\bullet-}$ is the rate-determining step (Scheme 2).[54]

The observed primary kinetic isotope effects (k_H/k_D) of the overall hydride transfer from $AcrH_2$ and the 9,9′-dideuterated compound ($AcrD_2$) to *p*-benzoquinone derivatives (Q) can be attributed to those of the proton transfer step from $AcrH_2^{\bullet+}$ and $AcrD_2^{\bullet+}$ to $Q^{\bullet-}$, since the variation of k_H/k_D with *p*-benzoquinone derivatives has been well correlated with the difference in the pK_a values between $AcrH_2^{\bullet+}$ and $QH^{\bullet}$ (pK_a), and the maximum value ($k_H/k_D = 10.4$) is obtained at $\Delta pK_a = 0$.[57]

In the course of hydride transfer reactions, an additional intermediate, that is, a CT complex is formed prior to the electron transfer step as indicated by the appearance of broad CT absorption band of the CT complex formed between AcrHR and A.[54] A negative temperature dependence was observed for the rates of hydride transfer reactions from AcrHR (R = H, Me, and CH_2Ph) to DDQ in chloroform (*the lower the temperature the faster the rate*) as shown in the Arrhenius plots (Fig. 2) to afford the negative activation enthalpy ($\Delta H^{\neq}_{obs} = -32$, -4, and -13 kJ mol^{-1}, respectively).[54] Such a negative $\Delta H^{\neq}_{obs}$ value indicates clearly that the CT complex lies along the reaction pathway of the hydride transfer reaction via sequential electron–proton–electron transfer and does not enter merely through a side reaction that has nothing to do with the hydride transfer reaction. The observed negative $\Delta H^{\neq}_{obs}$ values, which should be equal to $\Delta H_{CT} + \Delta H^{\neq}_1$ ($k_{obs} = k_1 K_{CT}$), could arise only when the CT complex lies along the reaction pathway. The heat of the formation of the CT complex ($\Delta H_{CT} < 0$) may be of greater magnitude than the activation enthalpy for the passage of the CT complex to the transition state ($\Delta H^{\neq}_1 > 0$, *i.e.*, $-\Delta H_{CT} > \Delta H^{\neq}_1$), when the $\Delta H^{\neq}_{obs}$ values ($\Delta H^{\neq}_{obs} = \Delta H_{CT} + \Delta H^{\neq}_1$) become negative. As demonstrated by a single correlation between log k_{obs} and log $k_d K_{et}$ in Fig. 1b, the $\Delta H^{\neq}_1$ value for the hydride transfer reaction consists of the sum of the activation enthalpies for electron transfer from AcrHR to DDQ in the CT complex and proton transfer from $AcrHR^{\bullet+}$ to $DDQ^{\bullet-}$ in the radical ion pair in Scheme 2.[54] Thus, the largest negative $\Delta H^{\neq}_{obs}$ value (-32 kJ mol^{-1}) is obtained for the reaction of $AcrH_2$ with DDQ when both electron transfer and proton transfer are fastest among the examined AcrHR and *p*-benzoquinone derivatives and the $\Delta H^{\neq}_1$ value is therefore minimized.[54]

When DDQ is replaced by a much weaker electron acceptor such as 1-(*p*-tolylsulfinyl)-2,5-benzoquinone (TolSQ), no reaction occurs between $AcrH_2$ and TolSQ in MeCN. In the presence of $HClO_4$, however, an efficient reduction of TolSQ by $AcrH_2$ occurs to yield $AcrH^+$ and $TolSQH_2$ (Eqn (6)).[58] The promoting effect of $HClO_4$ on the reduction of TolSQ by $AcrH_2$ results from protonation of TolSQ ($TolSQ + H^+ \rightarrow TolSQH^+$), which is confirmed by UV-Vis spectral changes of TolSQ in the presence of various concentrations of $HClO_4$.[58]

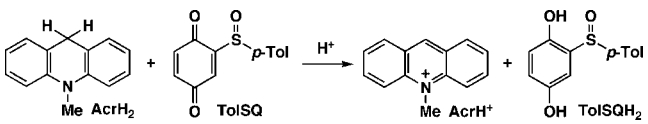

(6)

In the course of H^+-promoted hydride transfer from $AcrH_2$ to TolSQ, the formation of $AcrH_2^{\bullet+}$ is directly detected as a transient absorption band at $\lambda_{max} = 640$ nm (red line in Fig. 3a).[58] The formation of $AcrH_2^{\bullet+}$ was also confirmed by applying a rapid-mixing ESR technique, and the resulting ESR spectrum (Fig. 3b) agrees well with the computer simulation spectrum (Fig. 3c) of $AcrH_2^{\bullet+}$ with the hyperfine coupling constant (*hfc*) values [a_H (C-9) = 24.2, a_N (N—CH_3) = 14.0, a_H (N—CH_3) = 10.4, a_H (C-2,7) = 3.4, and a_H (C-4,5) = 1.0 G].[55,58,59] The *hfc* assignment in Fig. 3c was further confirmed by the deuterium substitution of two hydrogen atoms at the C-9 position of $AcrH_2$ because the observed ESR spectrum (Fig. 3d) agrees well with the computer simulation spectrum (Fig. 3e) using the same *hfc* values except for the value of the deuterium ($I = 1$) [a_D (C-9) = 3.7 G], which is reduced by the magnetogyric ratio of proton to deuterium (0.153).[55,58] The complete assignments of the ESR spectrum due to $AcrH_2^{\bullet+}$ observed in the thermal oxidation of $AcrH_2$ with $TolSQH^+$ strongly support the formation of $AcrH_2^{\bullet+}$ in the two-electron reduction of $TolSQH^+$ by $AcrH_2$ (Scheme 3).[58] However, there is no ESR signal due to $TolSQH^{\bullet}$ resulting from the electron transfer oxidation of $AcrH_2$ by $TolSQH^+$ (Fig. 3b), suggesting the rapid disproportionation of $TolSQH^{\bullet}$ (green arrow in Scheme 3).[58]

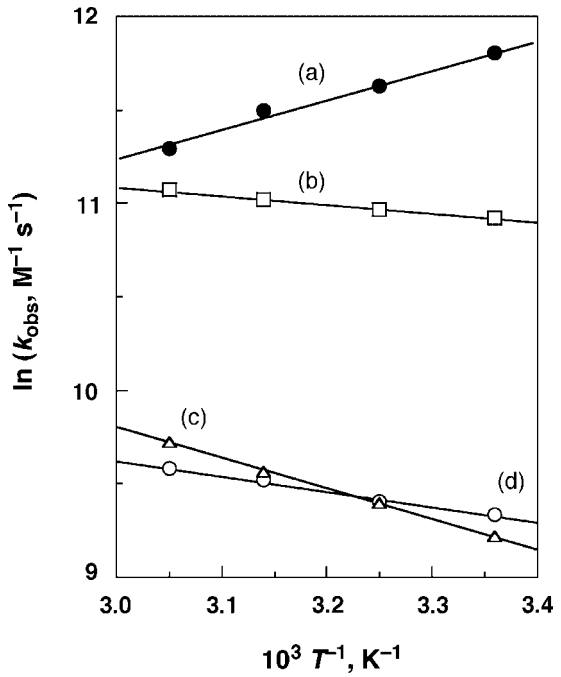

Figure 2. Arrhenius plots of k_{obs} for the reaction of $AcrHCH_2Ph$ (1.1×10^{-5} M) with DDQ (2.0×10^{-4} M) in (a) $CHCl_3$, (b) CH_2ClCH_2Cl, (c) PhCN, and (d) MeCN[54]

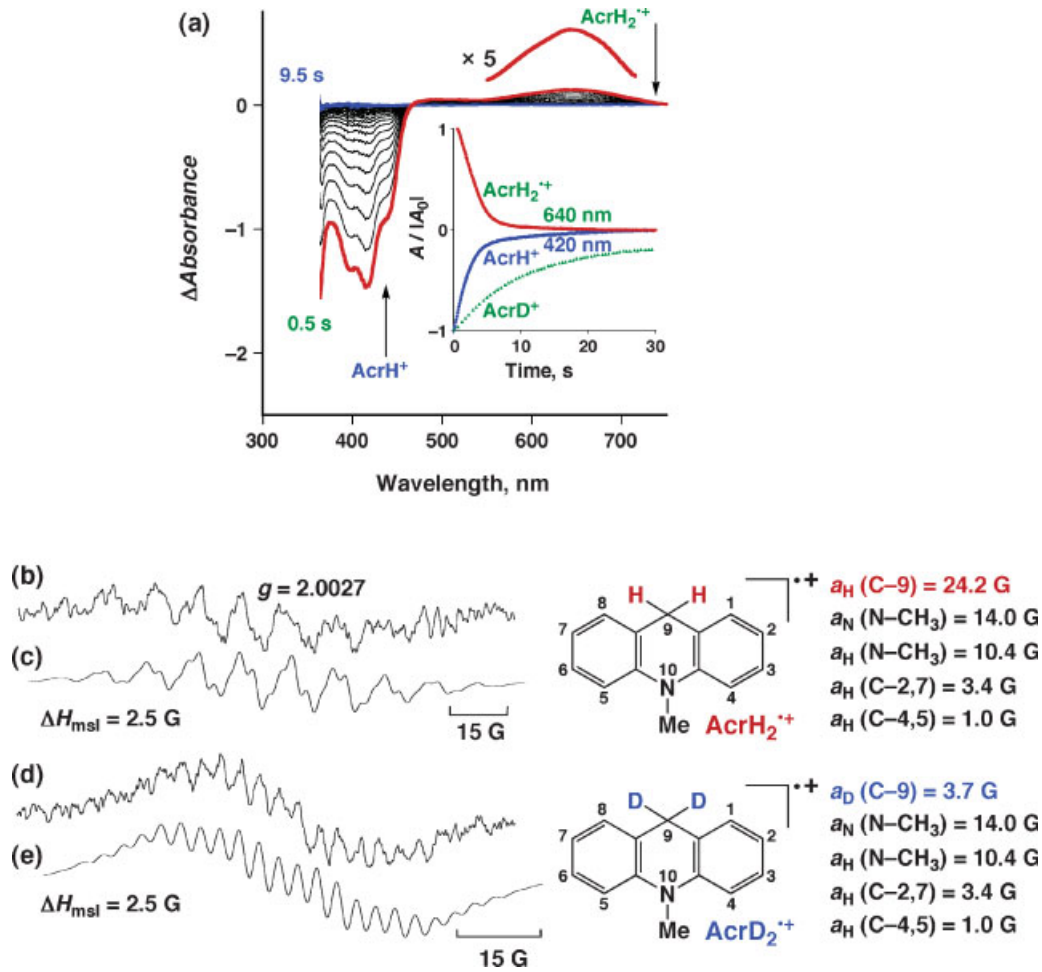

Figure 3. (a) Differential spectral changes in the reduction of TolSQ (4.6×10^{-4} M) by $AcrH_2$ (6.0×10^{-3} M) in the presence of $HClO_4$ (4.9×10^{-2} M) in deaerated MeCN at 298 K. Inset: Time course of the absorption change at $\lambda = 640$ nm (red) and $\lambda = 420$ nm (blue and green) for the reduction of TolSQ by $AcrH_2$ (red and blue circles) and $AcrD_2$ (green triangles), where A_0 is the initial absorbance.[58] (b) ESR spectrum of $AcrH_2^{+}$ generated by oxidation of $AcrH_2$ (2.9×10^{-3} M) with TolSQ (2.8×10^{-3} M) in the presence of $HClO_4$ (7.0×10^{-2} M) in deaerated MeCN at 298 K and (c) the computer simulation spectrum with the *hfc* values.[58] (d) ESR spectrum of $AcrD_2^{\cdot+}$ generated by oxidation of $AcrD_2$ (2.9×10^{-3} M) with TolSQ (2.8×10^{-3} M) in the presence of $HClO_4$ (7.0×10^{-2} M) in deaerated MeCN at 298 K and (e) the computer simulation spectrum with the *hfc* values[58,59]

In the absence of $HClO_4$, electron transfer from $AcrH_2$ ($E_{ox} = 0.81$ V *vs.* SCE)[55] to TolSQ ($E_{red} = -0.26$ V *vs.* SCE)[58] is highly endergonic because of the highly positive free energy change of electron transfer ($\Delta G_{et} = 1.07$ eV), and thereby no electron transfer reaction occurs. In the presence of $HClO_4$ (5.0×10^{-2} M), however, the one-electron reduction potential of TolSQ is shifted to 0.69 V *versus* SCE due to protonation of TolSQ.[58] The free energy change of electron transfer from $AcrH_2$ to $TolSQH^+$ is still slightly positive ($\Delta G_{et} = 0.12$ eV). In such a case, the efficient electron transfer from $AcrH_2$ to $TolSQH^+$ may be followed by rapid disproportionation of $TolSQH^{\cdot}$ (green arrow in Scheme 3), which makes the electron transfer reduction of $TolSQH^+$ exergonic.[58] The absorption at 640 nm due to $AcrH_2^{+}$ decays accompanied by the rise in absorption at 420 nm due to $AcrH^+$ as shown in Fig. 3a (red line–blue line).[58] The decay dynamics of $AcrH_2^{+}$ coincides with the rise dynamics of $AcrH^+$, exhibiting first-order and second-order processes (red and blue circles in Fig. 3a, inset), which correspond to the deprotonation and disproportionation of $AcrH_2^{+}$ as shown by blue and red solid arrows in Scheme 3, respectively.[58] Both first-order and

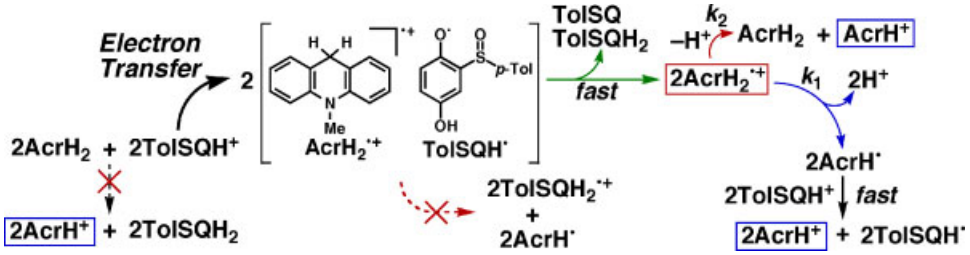

Scheme 3.

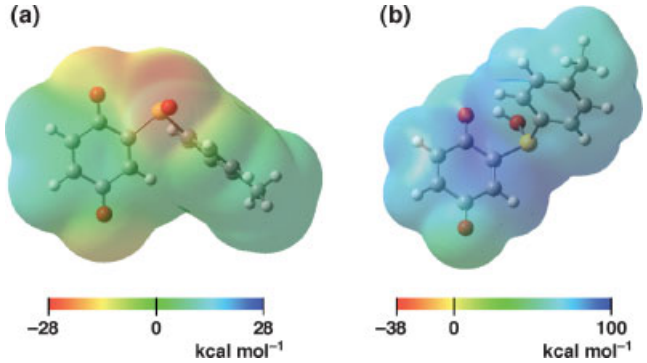

Figure 4. Electrostatic potential maps for (a) TolSQ and (b) $TolSQH^+$ calculated by using DFT at the BLYP/6-31G**[58]

second-order processes exhibit the primary kinetic isotope effects ($k_H/k_D = 3.2$ and 10, respectively) when $AcrH_2$ is replaced by the dideuterated compound ($AcrD_2$) (green triangles in Fig. 3a, inset).[58] Since $AcrH^•$ produced by deprotonation of $AcrH_2^+$ is a much stronger reductant than $AcrH_2$, the rapid electron transfer from $AcrH^•$ ($E_{ox} = -0.46$ V *vs.* SCE)[54] to $TolSQH^+$ occurs to produce $AcrH^+$ and $TolSQH^•$ (black solid arrow in Scheme 3).[58]

The reason why ET from $AcrH_2$ to $TolSQH^+$ occurs instead of the one-step hydride transfer is understood by examining the electrostatic potential map for $TolSQH^+$ (Fig. 4), which indicates that the positive charges (blue) due to protonation of TolSQ are fully delocalized over the entire ring systems (Fig. 4b) compared to TolSQ (Fig. 4a).[58] In such a case, the delocalization of positive charges (due to H^+) in $TolSQH^+$ results in a decrease in the electrophilicity of $TolSQH^+$, leading to deceleration of the one-step hydride transfer pathway. On the contrary, the electron transfer pathway is promoted by the protonation as indicated by the significant positive shift of the E_{red} value (*vide supra*).

DISCONTINUOUS CHANGE IN MECHANISMS BETWEEN ONE-STEP HYDRIDE TRANSFER AND STEPWISE ELECTRON TRANSFER PATHWAYS

Hydride transfer from $AcrH_2$ to TolSQ occurs efficiently both in the presence of Sc^{3+} and in the presence of H^+ (*vide supra*) to yield $AcrH^+$ and $TolSQH_2$ in deaerated MeCN at 298 K (Eqn (7)).[59] The dependence of the observed second-order rate constant (k_H) on

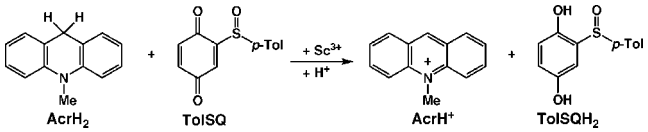

(7)

$[Sc^{3+}]$ is shown in Fig. 5a (red closed circles).[59] The k_H value increases with increasing Sc^{3+} concentration to reach a constant value ($k_H = 1.4 \times 10^3\ M^{-1}\ s^{-1}$).[59] The rates of hydride transfer exhibit a large primary kinetic isotope effect ($k_H/k_D = 5.3 \pm 0.1$) at low concentrations ($[Sc^{3+}] < 1.0 \times 10^{-2}$ M) when $AcrH_2$ is replaced by the dideuterated compound ($AcrD_2$).[59] In contrast to the case of $AcrH_2$, the observed second-order rate constant (k_D) increases linearly with an increase in $[Sc^{3+}]$ without exhibiting a saturation behavior at high concentrations ($[Sc^{3+}] > 1.0 \times 10^{-2}$ M) as shown in Fig. 5a (blue closed circles).[59] The primary kinetic isotope effect (k_H/k_D) therefore decreases with increasing $[Sc^{3+}]$ at high concentrations ($[Sc^{3+}] > 1.0 \times 10^{-2}$ M). The dependence of the observed second-order rate constants (k_H and k_D) on $[Sc^{3+}]$ is changed drastically when temperature is lowered to 233 K, where both k_H and k_D values increase linearly with increasing $[Sc^{3+}]$, exhibiting a primary kinetic isotope effect ($k_H/k_D = 2.6 \pm 0.2$) irrespective of Sc^{3+} concentration as shown in Fig. 5b (red and blue closed circles, respectively).[59]

The saturated dependence of k_H of hydride transfer from $AcrH_2$ to TolSQ (red closed circles in Fig. 5a) on $[Sc^{3+}]$ is ascribed to the 1:1 complex formation between TolSQ and Sc^{3+} (TolSQ–Sc^{3+}).[59] When hydride transfer from $AcrH_2$ to TolSQ proceeds via the TolSQ–Sc^{3+} complex, as shown in Scheme 4, the dependence of k_H on $[Sc^{3+}]$ is expressed by Eqn (8), which agrees with the experimental results in Fig. 5a (red line).

$$k_H = \frac{k_H^0 K[Sc^{3+}]}{1 + K[Sc^{3+}]} \quad (8)$$

The K values derived from Sc^{3+}-promoted hydride transfer reaction of $AcrH_2$ [$(2.3 \pm 0.1) \times 10^3\ M^{-1}$] agrees with that determined independently from UV-Vis spectral changes of TolSQ in the presence of various concentrations of Sc^{3+} [$K = (2.5 \pm 0.1) \times 10^3\ M^{-1}$] at 298 K.[59] Such agreement indicates

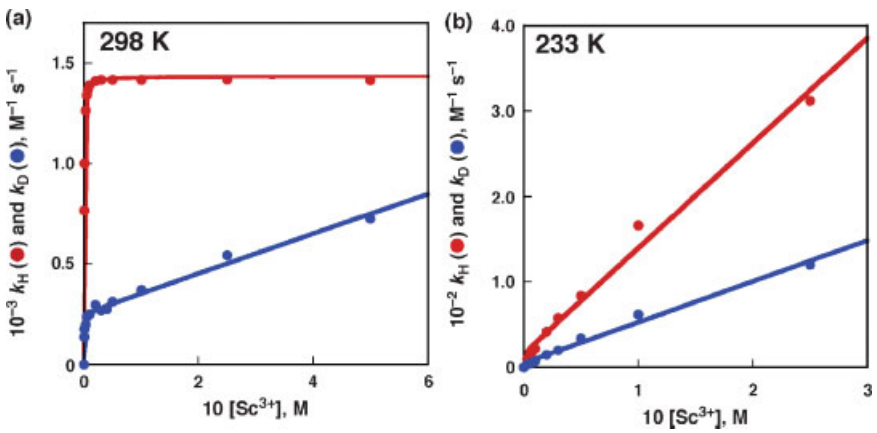

Figure 5. Dependence of k_H (●) and k_D (●) on $[Sc^{3+}]$ for hydride transfer from $AcrH_2$ (3.0×10^{-5} M) and $AcrD_2$ (3.0×10^{-5} M) to TolSQ in the presence of Sc^{3+} in deaerated MeCN at (a) 298 K and (b) 233 K[59]

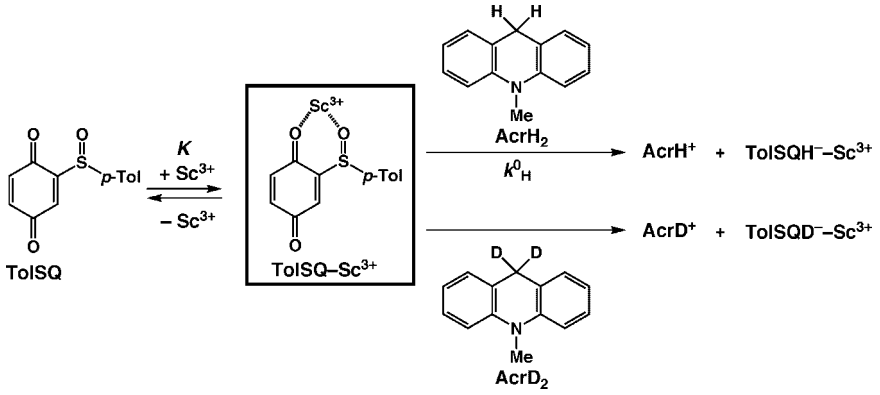

Scheme 4.

that the TolSQ–Sc^{3+} complex is indeed a reactive intermediate in Sc^{3+}-promoted hydride transfer from $AcrH_2$ to TolSQ, as shown in Scheme 4. In this case, hydride transfer from $AcrH_2$ to the TolSQ–Sc^{3+} complex occurs in a one-step pathway.

In contrast to the case of $AcrH_2$, the k_D value of $AcrD_2$ increases linearly with increasing Sc^{3+} concentration without exhibiting any saturation behavior at 298 K, although most TolSQ molecules form the Sc^{3+} complex in the high concentration range in Fig. 5a (blue closed circles).[59] At a lower temperature (233 K), both k_H and k_D values increase linearly with increasing [Sc^{3+}] without exhibiting any saturation behavior (Fig. 5b). Such dependence of k_D on [Sc^{3+}] in Fig. 5a is virtually the same as that observed in Sc^{3+}-promoted electron transfer reduction of TolSQ by tris(2-phenylpyridine)iridium [Ir(ppy)$_3$].[59] Thus, the hydride transfer mechanism is changed from one-step hydride transfer from $AcrH_2$ to the TolSQ–Sc^{3+} complex to Sc^{3+}-promoted electron transfer from $AcrD_2$ to the TolSQ–Sc^{3+} complex, as shown in Scheme 5.[59] The mechanistic changeover from the one-step hydride transfer to the electron transfer pathway by the deuterium substitution of $AcrH_2$ by $AcrD_2$ (Fig. 5a) results from a significant primary kinetic deuterium isotope effect in the direct one-step hydride transfer from $AcrD_2$ to the TolSQ–Sc^{3+} complex, when the rate constant of direct one-step hydride transfer from $AcrD_2$ becomes much smaller than that of the Sc^{3+}-promoted electron transfer from $AcrD_2$ to the TolSQ–Sc^{3+} complex.[59]

The electron transfer pathway in Scheme 5b is accelerated by the formation of Sc^{3+} complexes of semiquinone radical anion of TolSQ (TolSQ$^{\bullet-}$). A 1:1 complex with Sc^{3+} (TolSQ$^{\bullet-}$–Sc^{3+}) is detected by ESR in photoinduced electron transfer from 10,10′-dimethyl-9,9′-biacridine [(AcrH)$_2$][60] to the TolSQ–Sc^{3+} complex in deaerated MeCN at 298 K, as shown in Fig. 6a.[59] The ESR spectrum is well reproduced by the computer simulation spectrum with the *hfc* values of a(2H) = 1.85, 0.69 G and superhyperfine splitting due to one Sc^{3+} ion [a(Sc^{3+}) = 1.69 G] (Fig. 6b).[59] The 1:1 complex (TolSQ$^{\bullet-}$–Sc^{3+}) is converted to the 1:2 complex of TolSQ$^{\bullet-}$ with Sc^{3+} [TolSQ$^{\bullet-}$–(Sc^{3+})$_2$] at high concentration of Sc^{3+} as shown in Fig. 6c, where a drastic change in the hyperfine pattern is seen to exhibit further superhyperfine splitting due to additional Sc^{3+} ion (Fig. 6d).[59]

The temperature dependence of the hydride transfer reaction rates provides valuable insight into the mechanistic changeover in the hydride transfer reaction: one-step hydride transfer and electron transfer followed by proton–electron transfer. A plot of ln k_H *versus* T^{-1} for the hydride transfer reaction of $AcrH_2$ in the presence of high concentration of Sc^{3+} (2.5×10^{-1} M) is shown in Fig. 7a (open circles), where there are two segments in the temperature range of 233–298 K and 298–333 K with clearly different slopes.[59] In contrast, a single linear correlation is observed between ln k_H and T^{-1} for the hydride transfer reaction of $AcrH_2$ in the presence of low concentration of Sc^{3+} (1.0×10^{-2} M: closed squares in Fig. 7a).[59] In consequence, the k_H value in the presence of high concentration of Sc^{3+} (2.5×10^{-1} M: open circles) increases with increasing temperature to merge into the k_H values in the presence of low concentration of Sc^{3+} (1.0×10^{-2} M: closed squares). In contrast to the case of k_H in Fig. 7a, single linear correlations are observed between ln k_D and T^{-1} for the hydride transfer reactions of $AcrD_2$ in the presence of both low and high concentrations of Sc^{3+} (1.0×10^{-2} and 2.5×10^{-1} M), as shown in Fig. 7b (closed squares and open circles, respectively). Such differences in the temperature dependence of k_H and k_D on concentrations of Sc^{3+} result from the changeover of the reaction pathways between the one-step and multistep mechanisms.

The formation of a 1:2 complex between a radical anion and Sc^{3+} also plays an important role in the electron transfer pathway for Sc^{3+}-catalyzed hydride transfer from $AcrH_2$ to 3,6-diphenyl-1,2,4,5-tetrazine (Ph_2Tz), which contains N═N

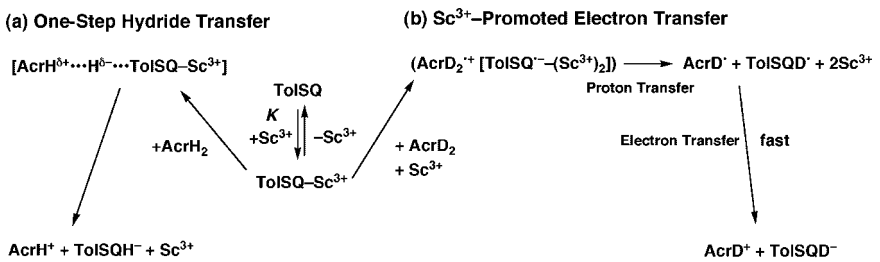

Scheme 5.

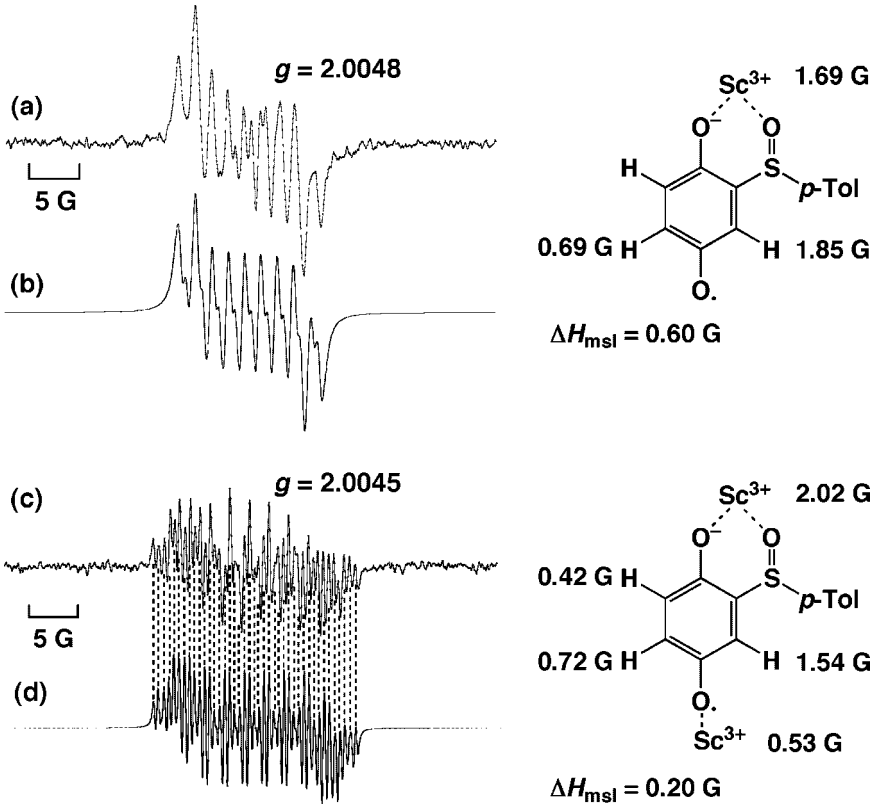

Figure 6. (a) ESR spectrum of $TolSQ^{\bullet-}$–Sc^{3+} produced by photoinduced electron transfer from $(AcrH)_2$ (1.6×10^{-2} M) to TolSQ (8.0×10^{-2} M) in the presence of Sc^{3+} (1.6×10^{-2} M) and H_2O (2.2 M) in deaerated MeCN at 298 K. (b) The computer simulation spectrum.[59] (c) ESR spectrum of $TolSQ^{\bullet-}$–$(Sc^{3+})_2$ produced by photoinduced electron transfer from $(AcrH)_2$ (1.6×10^{-2} M) to TolSQ (4.6×10^{-2} M) in the presence of Sc^{3+} (4.6×10^{-1} M) and H_2O (4.4 M) in deaerated MeCN at 298 K. (d) The computer simulation spectrum[59]

double bond (Eqn (9)).[62–64] The formation of 1:2 complex was confirmed by the

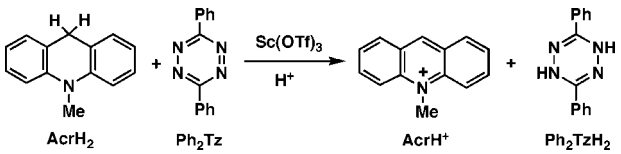

(9)

ESR spectrum in which the hyperfine structure is totally different from that of free $Ph_2Tz^{\bullet-}$ as shown in Fig. 8.[61] Electron transfer from $AcrH_2$ to Ph_2Tz is highly endergonic judging from the E_{ox} value of $AcrH_2$ (0.81 V)[55] and the E_{red} value of Ph_2Tz (−0.91 V)[61], and thus no reaction occurs between $AcrH_2$ and Ph_2Tz. In the presence of $Sc(OTf)_3$, however, the reduction potential of Ph_2Tz is shifted to a positive direction when electron transfer from $AcrH_2$ to Ph_2Tz becomes thermodynamically more feasible.[61]

CONTINUOUS CHANGE BETWEEN ONE-STEP AND STEPWISE PATHWAYS IN HYDROGEN TRANSFER REACTIONS OF NADH ANALOGUES

There is a mechanistic dichotomy of one-step *versus* stepwise pathways in hydrogen and hydride transfer reactions of NADH analogues (*vide supra*).[44–51] In the one-step mechanism, hydrogen transfer reaction occurs without an intermediate when electron and proton are transferred at the same time. Such reactions are generally regarded as proton-coupled electron transfer (PCET), and the definition of PCET encompasses both hydrogen atom transfer (HAT) and concerted electron and proton transfer.[62–71] A stepwise pathway consists of mechanistically distinct electron transfer and proton transfer steps involving a detectable intermediate. There has also been long standing ambiguity as to the mechanistic borderline where a one-step hydrogen transfer pathway is changed to a stepwise pathway or vice versa.[44–51]

The continuous change of mechanisms between a one-step hydrogen transfer pathway and a stepwise pathway has been delineated in the hydrogen transfer reactions of NADH analogues with the triplet excited states of tetrazines depending on the type of NADH analogues and tetrazines.[72] The triplet exited states of 3,6-disubstituted-tetrazines [R_2Tz: R = Ph (Ph_2Tz), 2-chlorophenyl [$(ClPh)_2Tz$], 2-pyridyl (Py_2Tz)] are produced by efficient energy transfer from $[Ru(bpy)_3^{2+}]^*$ (bpy = 2,2′-bipyridine, * denotes the excited state) to R_2Tz.[72] Whether formal hydrogen transfer from NADH analogues to $^3R_2Tz^*$ proceeds via a one-step or a stepwise pathway is changed by subtle difference in the electron donor ability and the deprotonation reactivity of the radical cations of NADH analogues as well as the electron-acceptor ability of $^3R_2Tz^*$ and the protonation reactivity of $R_2Tz^{\bullet-}$.[72]

In the case of $^3Ph_2Tz^*$, which is a weaker electron acceptor than the other tetrazine derivatives [$(ClPh)_2Tz$; Py_2Tz], direct one-step hydrogen transfer occurs from 10-methyl-9,10-dihydroacridine ($AcrH_2$) to $^3Ph_2Tz^*$ without the formation of the radical cation

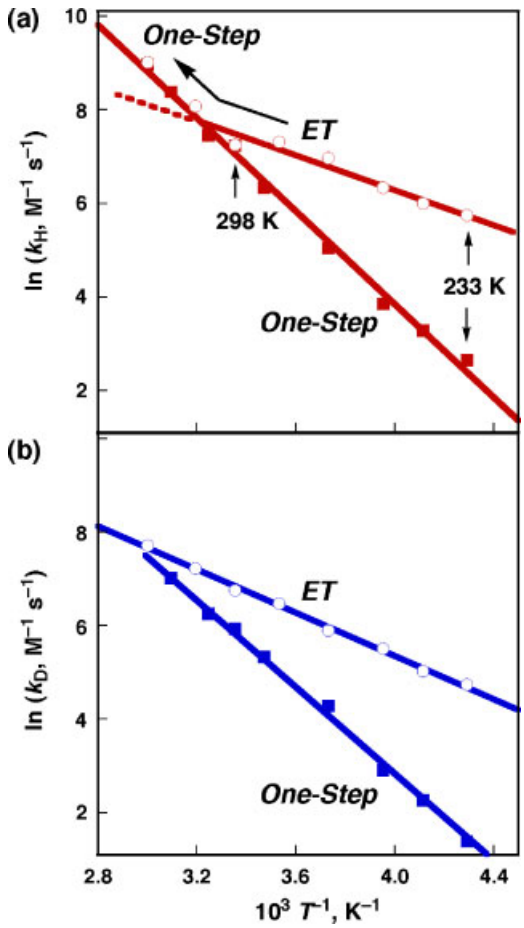

Figure 7. (a) Plots of ln k_H *versus* T^{-1} for hydride transfer from $AcrH_2$ (3.0×10^{-5} M) to TolSQ in the presence of $Sc(OTf)_3$ (1.0×10^{-2} M: ■, 2.5×10^{-1} M: ○) in deaerated MeCN.[59] (b) Plots of ln k_D *versus* T^{-1} for hydride transfer from $AcrD_2$ (3.0×10^{-5} M) to TolSQ in the presence of $Sc(OTf)_3$ (1.0×10^{-2} M: ■, 2.5×10^{-1} M: ○) in deaerated MeCN[59]

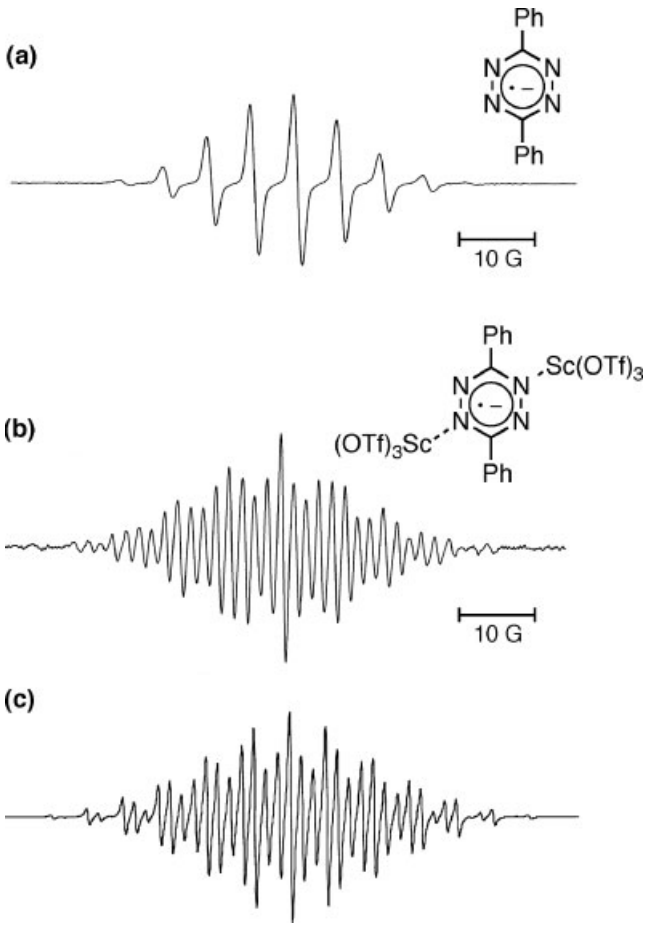

Figure 8. ESR spectrum of an MeCN solution containing $(BNA)_2$ (2.0×10^{-2} M) and Ph_2Tz (5.0×10^{-4} M) in the absence (a) and presence (b) of $Sc(OTf)_3$ (4.4×10^{-2} M) under irradiation with a high-pressure mercury lamp at 233 K.[61] (c) Computer simulation spectrum for (b) with $g = 2.0041$, $a(2N^1) = 6.6$ G, $a(2N^2) = 5.0$ G, $a(6H) = 5.0$ G, and $\Delta H_{msl} = 0.40$ G[61]

($AcrH_2^{+\cdot}$).[72] The laser flash photolysis of a deaerated MeCN solution of $Ru(bpy)_3^{2+}$ (4.6×10^{-5} M) at 450 nm in the presence of Ph_2Tz (9.6×10^{-5} M) and $AcrH_2$ (1.1×10^{-4} M) with 450 nm laser light results in the appearance of new absorption bands due to $AcrH^{\cdot}$ ($\lambda_{max} = 360$ and 520 nm)[73,74] with a concomitant decrease in the absorption band due to $^3Ph_2Tz^*$ ($\lambda_{max} = 535$ nm), as shown in Fig. 9, whereas no absorption band due to the $AcrH_2^{+\cdot}$ ($\lambda_{max} = 640$ nm)[55] is observed. Whether hydrogen transfer from $AcrH_2$ to $^3Ph_2Tz^*$ occurs via a one-step hydrogen transfer or a rate-determining electron transfer followed by fast proton transfer can be explained by examining the deuterium kinetic isotope effects. The one-step hydrogen transfer would afford a significant deuterium kinetic isotope effect, whereas the rate-determining electron transfer followed by fast proton transfer would exhibit no deuterium kinetic isotope effect. In fact, no deuterium kinetic isotope effect is observed in the emission quenching of $Ru(bpy)_3^{2+*}$ by $AcrH_2$, where electron transfer from $AcrH_2$ to $Ru(bpy)_3^{2+*}$ occurs as shown in Scheme 6a.[72] In contrast to the case of $Ru(bpy)_3^{2+*}$, the hydrogen transfer to $^3Ph_2Tz^*$ exhibits a significant primary deuterium kinetic isotope effect ($k_H/k_D = 1.80 \pm 0.20$; Fig. 10a,b).[72] In such a case, the hydrogen transfer from $AcrH_2$ to $^3Ph_2Tz^*$ occurs via a one-step process as

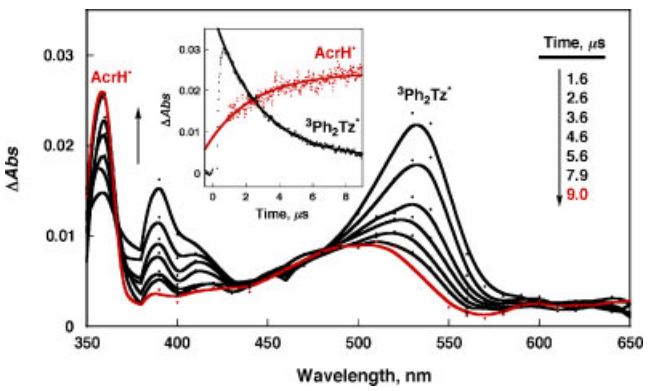

Figure 9. Transient absorption spectra observed by laser flash photolysis of a deaerated MeCN solution of $Ru(bpy)_3^{2+}$ (4.6×10^{-5} M) in the presence of $AcrH_2$ (1.1×10^{-4} M) and Ph_2Tz (9.6×10^{-4} M) at 1.6–9.0 μs after laser excitation at $\lambda = 450$ nm at 298 K. Inset: Time profile of the decay of absorbance at 535 nm due to $^3Ph_2Tz^*$ (black closed circles) and the rise of absorbance at 360 nm due to $AcrH^{\cdot}$ (red closed circles)[72]

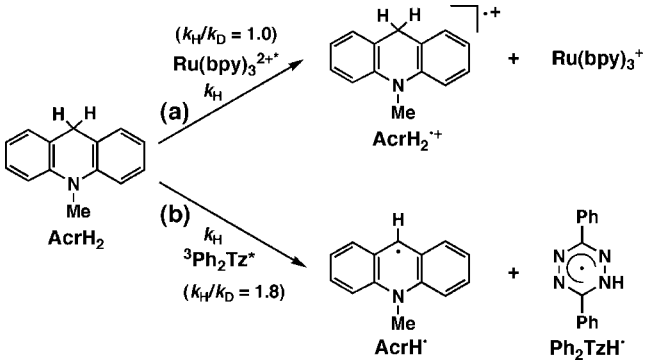

Scheme 6.

shown in Scheme 3b, which should be faster than electron transfer from $AcrH_2$ to $^3Ph_2Tz^*$.[73,74]

When $^3Ph_2Tz^*$ ($E_{red}^* = 1.09 \pm 0.04$ V *vs.* SCE) is replaced by a tetrazine derivative that has a slightly higher reduction potential of $^3(ClPh)_2Tz^*$ ($E_{red}^* = 1.11 \pm 0.05$ V *vs.* SCE), AcrH· is also generated by hydrogen transfer from $AcrH_2$ to $^3(ClPh)_2Tz^*$ without the formation of $AcrH_2^{+}$.[72] In contrast to the case of $^3Ph_2Tz^*$, a small primary kinetic isotope effect ($k_H/k_D = 1.11 \pm 0.08$) is observed (Fig. 10c,d).[72] This indicates that the one-step hydrogen transfer process is changed continuously to the stepwise pathway via electron transfer with a positive shift in the one-electron reduction potential of a tetrazine derivative. In fact, no deuterium kinetic isotope effect is observed (Fig. 10e), when $^3(ClPh)_2Tz^*$ ($E_{red}^* = 1.11 \pm 0.05$ V *vs.* SCE) is replaced by a tetrazine derivative, $^3Py_2Tz^*$ ($E_{red}^* = 1.25 \pm 0.04$ V *vs.* SCE), which has a stronger oxidizing ability than $^3(ClPh)_2Tz^*$.[72]

The replacement of the C(9)-H hydrogen of $AcrH_2$ by isopropyl group ($AcrHPr^i$) is known to retard deprotonation from $AcrHPr^{i\,\cdot+}$ because of the steric hindrance of the Pr^i group,[55] leading to the detection of $AcrHPr^{i\,\cdot+}$ in the stepwise electron and proton transfer.[72] The laser flash excitation (450 nm) of a deaerated MeCN solution of $Ru(bpy)_3^{2+}$ (4.6×10^{-5} M) and $AcrHPr^i$ (8.8×10^{-4} M) in the presence of $(ClPh)_2Tz$ (9.6×10^{-4} M) results in the formation of $AcrHPr^{i\,\cdot+}$ ($\lambda_{max} = 680$ nm)[55] as shown in Fig. 11a.[72] The time profiles of the transient absorption at 530 nm due to $^3(ClPh)_2Tz^*$, at 680 nm due to $AcrHPr^{i\,\cdot+}$, and at 510 nm due to $AcrPr^{i\,\cdot}$ are shown in Fig. 11b.[72] The absorption at 530 nm due to $^3(ClPh)_2Tz^*$ decays immediately within 2 μs after laser excitation, accompanied by the rise in absorption at 680 nm due to $AcrHPr^{i\,\cdot+}$. The decay of absorbance at 680 nm due to $AcrHPr^{i\,\cdot+}$ coincides with the rise in absorbance at 510 nm due to $AcrPr^{i\,\cdot}$ (Fig. 11b). This indicates that electron transfer from $AcrHPr^i$ to $^3(ClPh)_2Tz^*$ occurs rapidly to produce $AcrHPr^{i\,\cdot+}$ and $(ClPh)_2Tz^{\cdot-}$ within 2 μs, followed by the slower proton transfer from $AcrHPr^{i\,\cdot+}$ to $(ClPh)_2Tz^{\cdot-}$ to produce $AcrPr^{i\,\cdot}$ (Fig. 11a) as shown in Scheme 7.[72]

When $AcrH_2$ is replaced by BNAH that is a stronger electron donor than $AcrH_2$,[37] the one-step hydrogen transfer pathway in Scheme 6b is also changed to the stepwise electron transfer pathway: electron transfer from BNAH to $^3Ph_2Tz^*$ to produce $BNAH^{\cdot+}$ and $Ph_2Tz^{\cdot-}$, followed by proton transfer from $BNAH^{\cdot+}$ to $Ph_2Tz^{\cdot-}$ to yield BNA·.[72] Each step can be followed by the laser flash photolysis measurements in comparison with the transient absorption spectrum of $BNAH^{\cdot+}$, which was produced by the ET oxidation of BNAH with $Ru(bpy)_3^{3+}$ [75]. In this case, there is no primary isotope effect ($k_H/k_D = 1.0 \pm 0.1$) in the quenching process of $^3R_2Tz^*$ by BNAH when BNAH is replaced by BNAH-4,4′-d_2.[72]

Thus, the reactions of NADH analogues with $^3R_2Tz^*$ occur via one-step hydrogen transfer, the rate-limiting electron transfer followed by fast proton transfer or sequential electron–proton transfer depending on the electron-donor ability of NADH analogues as well as the electron-acceptor ability of $^3R_2Tz^*$ and the protonation reactivity of $R_2Tz^{\cdot-}$.[72]

SUMMARY AND CONCLUSIONS

As demonstrated in this review, hydride transfer reactions from NADH analogues, 10-methyl-9,10-dihydroacridine ($AcrH_2$) as well as 1-benzyl-1,4-dihydronicotinamide (BNAH), to hydride acceptors (A) that are strong electron acceptors such as TCNE and DDQ occur via sequential electron–proton–electron transfer through CT complexes formed between NADH analogues and acceptors. Enhancement of the electron-acceptor ability of TolSQ by protonation results in electron transfer from NADH analogues to $TolSQH^+$ in preference to one-step hydride transfer, because the delocalization of the positive charges (due to H^+) in $TolSQH^+$ leads to a decrease in the electrophilicity of $TolSQH^+$. The one-step

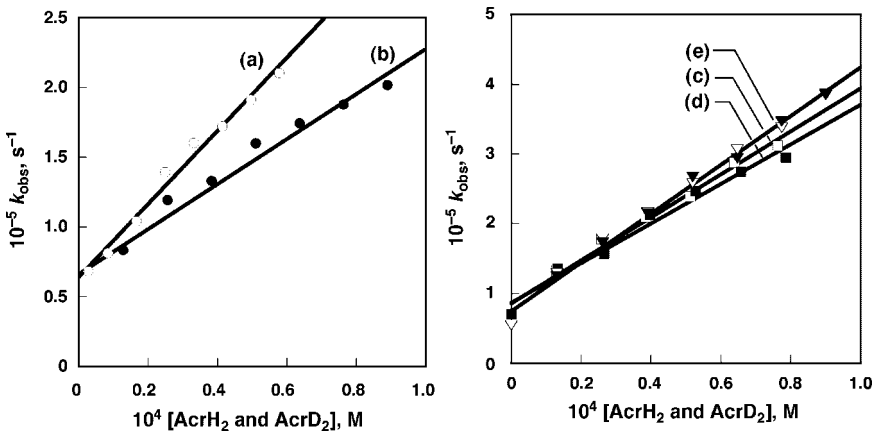

Figure 10. Plots of k_{obs} *versus* [$AcrH_2$] and [$AcrD_2$] for the reactions of $^3Ph_2Tz^*$ with (a) $AcrH_2$ (○) and (b) $AcrD_2$ (●), the reactions of $^3(ClPh)_2Tz^*$ with (c) $AcrH_2$ (□) and (d) $AcrD_2$ (■), and (e) the reactions of $^3Py_2Tz^*$ with $AcrH_2$ (▽) and $AcrD_2$ (▼) in deaerated MeCN at 298 K[72]

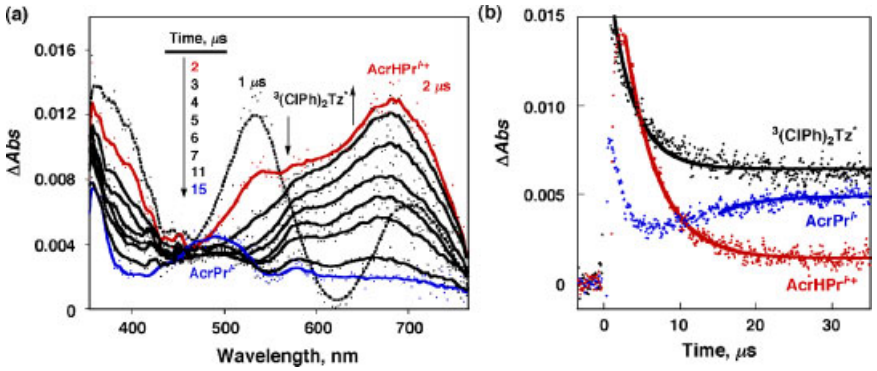

Figure 11. (a) Transient absorption spectra observed by laser flash photolysis of a deaerated MeCN solution of $Ru(bpy)_3^{2+}$ (4.6×10^{-5} M) in the presence of $AcrHPr^i$ (8.8×10^{-4} M) and $(ClPh)_2Tz$ (9.6×10^{-4} M) at 1–15 μs after laser excitation at $\lambda = 450$ nm at 298 K.[72] (b) Time profiles of the decay of absorbance at 530 nm due to $^3(ClPh)_2Tz^*$, the decay of absorbance at 680 nm due to $AcrHPr^{i\cdot+}$ and the rise of absorbance at 510 nm due to $AcrPr^{i\cdot}$.[72]

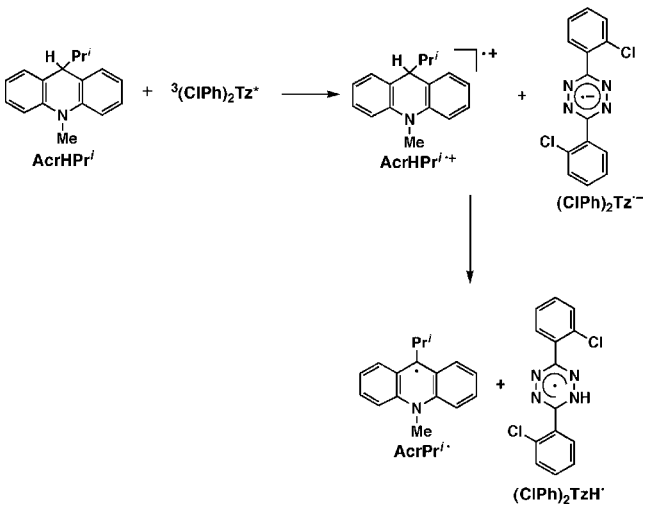

Scheme 7.

hydride transfer pathway in the Sc^{3+}-promoted hydride transfer from $AcrH_2$ to TolSQ is changed to the stepwise electron transfer pathway by deuterium substitution of $AcrH_2$ with $AcrD_2$ and also by decreasing temperature. The borderline between the one-step hydride transfer and electron transfer pathways is shown as a break in the Arrhenius plot. In this case, one-step hydride transfer and electron transfer pathways are employed simultaneously. In contrast to this, a one-step hydrogen transfer pathway is changed continuously to the rate-limiting electron transfer followed by fast proton transfer in hydrogen transfer from an NADH analogue to the triplet excited state of tetrazine derivatives with increasing electron-acceptor ability of tetrazine derivatives. The scope and the applications of fine control on the mechanisms of hydride and hydrogen transfer reactions of NADH analogues are expected to expand much further in the future.

Acknowledgements

The authors gratefully acknowledge the contributions of their collaborators and coworkers mentioned in the references. The authors acknowledge continuous support of their study by Grants-in-Aid from the Ministry of Education, Culture, Sports, Science and Technology, Japan.

REFERENCES

[1] L. Stryer, *Biochemistry*, 3rd ed. Freeman, New York, **1988**. Chapter 17.
[2] S. Fukuzumi, *Advances in Electron Transfer Chemistry* (Ed.: P. S. Mariano), JAI Press, Greenwich, CT, **1992**. pp. 67–175.
[3] S. Fukuzumi, T. Tanaka, *Photoinduced Electron Transfer* (Eds.: M. A. Fox, M. Chanon), Elsevier, Amsterdam, **1988**. Part C; Chap. 10.
[4] S. Fukuzumi, S. Itoh, *Antioxid. Redox Signal.* **2001**, *3*, 807–824.
[5] X. Q. Zhu, Y. Yang, M. Zhang, J. P. Cheng, *J. Am. Chem. Soc.* **2003**, *125*, 15298–15299.
[6] B. W. Carlson, L. L. Miller, P. Neta, J. Grodkowski, *J. Am. Chem. Soc.* **1984**, *106*, 7233–7239.
[7] M. F. Powell, J. C. Wu, T. C. Bruice, *J. Am. Chem. Soc.* **1984**, *106*, 3850–3856.
[8] A. Sinha, T. C. Bruice, *J. Am. Chem. Soc.* **1984**, *106*, 7291–7292.
[9] T. Matsuo, J. M. Mayer, *Inorg. Chem.* **2005**, *44*, 2150–2158.
[10] A. S. Larsen, K. Wang, M. A. Lockwood, G. L. Rice, T. J. Won, S. Lovell, M. Sadílek, F. Turecek, J. M. Mayer, *J. Am. Chem. Soc.* **2002**, *124*, 10112–10123.
[11] O. Pestovsky, A. Bakac, J. H. Espenson, *J. Am. Chem. Soc.* **1998**, *120*, 13422–13428.
[12] O. Pestovsky, A. Bakac, J. H. Espenson, *Inorg. Chem.* **1998**, *37*, 1616–1622.
[13] M. Afanasyeva, M. B. Taraban, P. A. Purtov, T. V. Leshina, C. B. Grissom, *J. Am. Chem. Soc.* **2006**, *128*, 8651–8658.
[14] S. Fukuzumi, Y. Kondo, T. Tanaka, *J. Chem. Soc., Perkin Trans.* **1984**, *2*, 673–679.
[15] W. W. Ellis, J. W. Raebiger, C. J. Curtis, J. W. Bruno, D. L. DuBois, *J. Am. Chem. Soc.* **2004**, *126*, 2738–2743.
[16] I. S. H. Lee, E. H. Jeoung, M. M. Kreevoy, *J. Am. Chem. Soc.* **1997**, *119*, 2722–2728.
[17] M. F. Powell, T. C. Bruice, *J. Am. Chem. Soc.* **1983**, *105*, 1014–1021.
[18] A. Ohno, H. Yamamoto, S. Oka, *J. Am. Chem. Soc.* **1981**, *103*, 2041–2045.
[19] A. Ohno, T. Shio, H. Yamamoto, S. Oka, *J. Am. Chem. Soc.* **1981**, *103*, 2045–2048.
[20] D. D. Tanner, A. Kharrat, H. Oumar-Mahamat, *Can. J. Chem.* **1990**, *68*, 1662–1677.
[21] Y. Kim, D. G. Truhlar, M. M. Kreevoy, *J. Am. Chem. Soc.* **1991**, *113*, 7837–7847.
[22] M. M. Kreevoy, A. T. Kotchevar, *J. Am. Chem. Soc.* **1990**, *112*, 3579–3583.
[23] A. Anne, J. Moiroux, *J. Org. Chem.* **1990**, *55*, 4608–4614.
[24] A. Anne, J. Moiroux, J. M. Savéant, *J. Am. Chem. Soc.* **1993**, *115*, 10224–10230.

[25] S. Fukuzumi, N. Nishizawa, T. Tanaka, *J. Org. Chem.* **1984**, *49*, 3571–3578.
[26] S. Fukuzumi, M. Ishikawa, T. Tanaka, *J. Chem. Soc., Perkin Trans.* **1989**, *2*, 1037–1045.
[27] S. Fukuzumi, S. Mochizuki, T. Tanaka, *J. Am. Chem. Soc.* **1989**, *111*, 1497–1499.
[28] S. Fukuzumi, T. Kitano, M. Ishikawa, *J. Am. Chem. Soc.* **1990**, *112*, 5631–5632.
[29] B. W. Carlson, L. L. Miller, *J. Am. Chem. Soc.* **1985**, *107*, 479–485.
[30] L. L. Miller, J. R. Valentine, *J. Am. Chem. Soc.* **1988**, *110*, 3982–3989.
[31] A. K. Colter, P. Plank, J. P. Bergsma, R. Lahti, A. A. Quesnel, A. G. Parsons, *Can. J. Chem.* **1984**, *62*, 1780–1784.
[32] C. A. Coleman, J. G. Rose, C. J. Murray, *J. Am. Chem. Soc.* **1992**, *114*, 9755–9762.
[33] C. J. Murray, T. Webb, *J. Am. Chem. Soc.* **1991**, *113*, 7426–7427.
[34] H. Sund, *Pyridine-Nucleotide Dependent Dehydrogenase*, Walter de Gruyer, West Berlin, **1977**.
[35] R. M. Kellog, *Top. Curr. Chem.* **1982**, *101*, 111–145.
[36] D. S. Sigman, J. Hajdu, D. J. Creighton, In: *Bioorganic Chemistry*, Vol. *IV*(Ed.: E. E. van Tamelen), Academic Press, New York, **1978**. p. 385.
[37] S. Fukuzumi, S. Koumitsu, K. Hironaka, T. Tanaka, *J. Am. Chem. Soc.* **1987**, *109*, 305–316.
[38] M. Ishikawa, S. Fukuzumi, *J. Chem. Soc., Faraday Trans.* **1990**, *86*, 3531–3536.
[39] S. Fukuzumi, N. Nishizawa, T. Tanaka, *J. Chem. Soc., Perkin Trans.* **1985**, *2*, 371–378.
[40] S. Fukuzumi, K. Ohkubo, T. Okamoto, *J. Am. Chem. Soc.* **2002**, *124*, 14147–14155.
[41] S. Fukuzumi, Y. Fujii, T. Suenobu, *J. Am. Chem. Soc.* **2001**, *123*, 10191–10199.
[42] R. Reichenbach-Klinke, M. Kruppa, B. König, *J. Am. Chem. Soc.* **2002**, *124*, 12999–13007.
[43] S. Fukuzumi, K. Hironaka, T. Tanaka, *J. Am. Chem. Soc.* **1983**, *105*, 4722–4727.
[44] C. G. Schaefer, K. S. Peters, *J. Am. Chem. Soc.* **1980**, *102*, 7566–7567.
[45] K. S. Peters, E. Pang, J. Rudzki, *J. Am. Chem. Soc.* **1982**, *104*, 5535–5537.
[46] L. E. Manring, K. S. Peters, *J. Am. Chem. Soc.* **1983**, *105*, 5708–5709.
[47] S. C. Freilich, K. S. Peters, *J. Am. Chem. Soc.* **1985**, *107*, 3819–3822.
[48] J. M. Mayer, *Annu. Rev. Phys. Chem.* **2004**, *55*, 363–390.
[49] J. M. Hodgkiss, J. Rosenthal, D. G. Nocera, In: *Hydrogen-Transfer Reactions*, Vol. *2*(Ed.: J. T. Hybes), Wiley-VCH, Weinheim, **2007**. pp. 503–562.
[50] M. Sjodin, S. Styring, H. Wolpher, Y. Xu, L. Sun, L. Hammarstrom, *J. Am. Chem. Soc.* **2005**, *127*, 3855–3863.
[51] M. Sjodin, S. Styring, B. Akermark, L. Sun, L. Hammarstrom, *J. Am. Chem. Soc.* **2000**, *122*, 3932–3936.
[52] A. K. Colter, G. Saito, F. J. Sharom, A. P. Hong, *J. Am. Chem. Soc.* **1976**, *98*, 7833–7835.
[53] A. K. Colter, G. Saito, F. J. Sharom, *Can. J. Chem.* **1977**, *55*, 2741–2751.
[54] S. Fukuzumi, K. Ohkubo, Y. Tokuda, T. Suenobu, *J. Am. Chem. Soc.* **2000**, *122*, 4286–4294.
[55] S. Fukuzumi, Y. Tokuda, T. Kitano, T. Okamoto, J. Otera, *J. Am. Chem. Soc.* **1993**, *115*, 8960–8968.
[56] S. Fukuzumi, Y. Tokuda, *J. Phys. Chem.* **1992**, *96*, 8409–8413.
[57] M. Ishikawa, S. Fukuzumi, *J. Chem. Soc., Faraday Trans.* **1990**, *86*, 3531–3536.
[58] J. Yuasa, S. Yamada, S. Fukuzumi, *Angew. Chem. Int. Ed.* **2008**, *47*, 1068–1071.
[59] J. Yuasa, S. Yamada, S. Fukuzumi, *J. Am. Chem. Soc.* **2006**, *128*, 14938–14948.
[60] S. Fukuzumi, T. Kitano, K. Mochida, *J. Am. Chem. Soc.* **1990**, *112*, 3246–3247.
[61] S. Fukuzumi, J. Yuasa, T. Suenobu, *J. Am. Chem. Soc.* **2002**, *124*, 12566–12573.
[62] J. M. Mayer, I. J. Rhile, *Biochim. Biophys. Acta* **2004**, *1655*, 51–58.
[63] J. R. Bryant, J. M. Mayer, *J. Am. Chem. Soc.* **2003**, *125*, 10351–10361.
[64] J. P. Roth, J. C. Yoder, T. J. Won, J. M. Mayer, *Science* **2001**, *294*, 2524–2526.
[65] R. I. Cukier, D. G. Nocera, *Annu. Rev. Phys. Chem.* **1998**, *49*, 337–369.
[66] J. Stubbe, D. G. Nocera, C. S. Yee, M. C. Y. Chang, *Chem. Rev.* **2003**, *103*, 2167–2202.
[67] C. J. Chang, M. C. Y. Chang, N. H. Damrauer, D. G. Nocera, *Biochim. Biophys. Acta* **2004**, *1655*, 13–28.
[68] A. Kohen, J. P. Klinman, *Acc. Chem. Res.* **1998**, *31*, 397–404.
[69] S. Hammes-Schiffer, *Acc. Chem. Res.* **2001**, *34*, 273–281.
[70] C. Isborn, D. A. Hrovat, W. T. Borden, J. M. Mayer, B. K. Carpenter, *J. Am. Chem. Soc.* **2005**, *127*, 5794–5795.
[71] J. M. Mayer, D. A. Hrovat, J. L. Thomas, W. T. Borden, *J. Am. Chem. Soc.* **2002**, *124*, 11142–11147.
[72] J. Yuasa, S. Fukuzumi, *J. Am. Chem. Soc.* **2006**, *128*, 14281–14292.
[73] K. Ohkubo, K. Suga, K. Morikawa, S. Fukuzumi, *J. Am. Chem. Soc.* **2003**, *125*, 12850–12859.
[74] S. Fukuzumi, K. Ohkubo, T. Suenobu, K. Kato, M. Fujitsuka, O. Ito, *J. Am. Chem. Soc.* **2001**, *123*, 8459–8467.
[75] S. Fukuzumi, O. Inada, T. Suenobu, *J. Am. Chem. Soc.* **2003**, *125*, 4808–4816.